Smart Structures and Systems, *Vol. 15, No. 1 (2015) 119-133*
DOI: http://dx.doi.org/10.12989/sss.2015.15.1.119

Structural time-varying damage detection using synchrosqueezing wavelet transform

Jing-Liang Liu[1a], Zuo-Cai Wang[2b], Wei-Xin Ren[*1,2] and Xing-Xin Li[2c]

[1]*School of Civil Engineering, Central South University, Changsha, People's Republic of China*
[2]*School of Civil and Hydraulic Engineering, Hefei University of Technology, Hefei, People's Republic of China*

(Received January 20, 2014, Revised May 25, 2014, Accepted June 10, 2014)

Abstract. This paper proposed a structural time-varying damage detection method by using synchrosqueezing wavelet transform. The instantaneous frequencies of a structure with time-varying damage are first extracted using the synchrosqueezing wavelet transform. Since the proposed synchrosqueezing wavelet transform is invertible, thus each individual component can be reconstructed and the modal participation factor ratio can be extracted based on the amplitude of the analytical signals of the reconstructed individual components. Then, the new time-varying damage index is defined based on the extracted instantaneous frequencies and modal participation factor ratio. Both free and forced vibrations of a classical Duffing nonlinear system and a simply supported beam structure with abrupt and linear time-varying damage are simulated. The proposed synchrosqueezing wavelet transform method can successfully extract the instantaneous frequencies of the damaged structures under free vibration or vibration due to earthquake excitation. The results also show that the defined time-varying damage index can effectively track structural time-varying damage.

Keywords: synchrosqueezing wavelet transform; instantaneous frequency; modal participation factor ratio; time-varying damage detection

1. Introduction

Civil engineering structures often suffer local or global damage when they are subjected to earthquakes, tornados and other extreme loads. The structural damage causes structural dynamic characteristic properties vary over time and leads to non-stationary responses. Moreover, during the oscillation, the degree of structural damage usually varies from minor to severe. To track the structural damage evolution during the vibration, it is quite necessary to identify the time-varying structural parameters such as instantaneous modal frequencies and mode shapes from the measured responses.

In recent years, identification of time-varying structures and damage detection based on time-frequency representation (TFR) analysis method has been attracting wide attention. Various

*Corresponding author, Professor, E-mail: renwx@hfut.edu.cn
[a] Ph.D. Student, E-mail: zfcljl@163.com
[b] Professor, E-mail: wangzuocai1127@163.com
[c] Ph.D., E-mail: lstar@hfut.edu.cn

http://www.techno-press.org/?journal=sss&subpage=8 ISSN: 1738-1584 (Print), 1738-1991 (Online)

time-frequency methods proposed in literature include short-time Fourier transform (STFT), Gabor transform, Cohen class quadratic distribution, Hilbert-Huang transform (HHT) (Huang *et al*. 1998, 1999) and continuous wavelet transform (CWT) (Kijewski and Kareem 1999, 2007). Among the above mentioned methods, HHT and CWT play the most important role without adding more complexity. Huang et al. (1998) explored a sifting procedure called empirical modal decomposition (EMD) to decompose a multi-component signal into several intrinsic mode functions (IMFs), then Hilbert spectral analysis was employed to realize the extraction of instantaneous characteristics of non-stationary signals. To solve mode mixing problem in EMD, Wu and Huang (2009) further developed ensemble empirical modal decomposition (EEMD). Over the last two decades, HHT has been successfully applied in many engineering fields. However, since HHT belongs to empirical analysis method, it still encounters a few problems in practical application, for example, HHT still have some difficulties in negative frequency, distortion, non-convergence EMD and the ambiguity of IMF definition (Huang *et al*. 2005). In addition, HHT can't decompose a signal with overlapping modal frequencies (Chen and Wang 2012).

Wavelet transform as one of the time-frequency analysis tools has attracted wide attention in recent years. Ruzzene *et al*. (1997) introduced complex wavelet transform to estimate natural frequencies and viscous damping ratios from responses of both free and ambient vibrations. Hou *et al*. (2006) employed a wavelet-based structural health monitoring technique to extract instantaneous mode shapes from the responses due to earthquake excitations. More recently, Xu and Shi (2012) combined wavelet theory and state-space method for the identification of dynamic parameters in linear time-varying system. Although wavelet transform has been widely used in time-varying parameter identification or damage detection, Kijewski and Kareem (2003) pointed out that wavelet transform can't always provide finer enough frequency resolution for long period signal components which is marked for vibration response of civil engineering structures. Therefore, how to get a clear view of time-frequency curves about measured signal remains a problem to be resolved.

More recently, Daubechies *et al*. (2012) explored a new wavelet based time-frequency method named synchrosqueezing wavelet transform, which is a combination of wavelet analysis and reallocation method. Their proposed method can effectively reassign time frequency curves to get more accurate results, and decompose an arbitrary signal to a linear superposition of several approximate harmonics at ease. Wu *et al*. (2011) presented an EMD-inspired synchrosqueezing method to extract close spaced instantaneous frequencies. Li and Liang (2012a,b) proposed a generalized synchrosqueezing transform (GST) approach to detect and diagnose gearbox faults due to the diffusions of the TFR energy along time or frequency axes. Although the developed synchrosqueezing wavelet transform is powerful to extract instantaneous frequencies of signals and reconstruct individual signal components, practical applications are still relatively rare, especially in the field of civil engineering.

Civil engineering structures are prone to damage even failure when they are subjected to earthquakes or other extreme loads. Structural damage often causes changes in physical parameters, such as stiffness, damping and mass. These changes in physical parameters in turn affect the dynamic behavior of the structure. In the last few decades, vibration based damage detection methods have attracted tremendous amount of attention (Yan *et al*. 2007, Kopsaftopoulos and Fassois 2013). The basic idea of these methods is that modal parameters are functions of physical properties. Any damage such as stiffness reduction may cause detectable changes in frequency, mode shapes and so on. Recently, the wavelet transform based time-frequency analysis methods were developed for civil structural damage detection. For instance, Rucka (2011) dealt with the wavelet-based damage detection technique on a cantilever beam. Golmohamadi *et al*. (2012) proposed an effective method for damage estimation based on statistical moments of the energy density function of the vibration response in the time-frequency domain by using CWT.

In this paper, synchrosqueezing wavelet transform is introduced to estimate instantaneous frequencies of structures with time-varying damage. A nonlinear Duffing system with free and forced vibrations is simulated as numerical examples to validate the accuracy and effectiveness of the method. The estimated instantaneous frequencies can be directly employed to detect the presence and the quantification of damage severity. However, frequency as a damage index only relates well with the change of global stiffness but is less sensitive to local stiffness reduction (Doebling *et al*. 1998, Yang and Wang 2010, Fayyadh *et al*. 2011). On the other hand, mode shapes and its derivatives are more promising in the detection of both location and degree of damage. To effectively detect the structural damage, combined indices of natural frequency and mode shape are more widely used (Pandey and Biswas 1994, Jaishi and Ren 2006, Yan *et al*. 2006, Yang and Liu 2006, Wang and Lin 2007). In this study, a new time-varying damage index is defined, which just needs to know the instantaneous frequency and the modal participation factor ratio and does not require mass normalized mode shape. The effectiveness of this new damage index is validated by a numerical simply supported beam with abrupt and linear time-varying damage, while the accuracy of instantaneous frequency is verified by a nonlinear Duffing system.

2. Theoretical background

2.1 Continues wavelet transform

Wavelet transform is a time-frequency signal processing method which relies on the introduction of an appropriate basis. Detailed information regarding wavelet transform and its application can be found in (Mallat 1999). For a given parent wavelet function $\psi(t)$, that is $\psi(t) \in L^2(R)$, a family of wavelet $\psi_{a,b}(t)$ is generated by dilations and translations of itself,

$$\psi_{a,b}(t) = \frac{1}{\sqrt{a}}\, \psi\left(\frac{t-b}{a}\right) \tag{1}$$

where a is a scale factor which plays the role of the inverse of frequency, and b is a translation factor related to time. The CWT of any signal $x(t)$ is defined by

$$W_x(a,b) = \int_{-\infty}^{\infty} x(t)\frac{1}{\sqrt{a}}\overline{\psi\left(\frac{t-b}{a}\right)}\, \mathrm{d}t \tag{2}$$

in which $\overline{\psi\left(\frac{t-b}{a}\right)}$ represents the complex conjugate of a family of wavelet $\psi\left(\frac{t-b}{a}\right)$. Wavelet coefficients $W_x(a,b)$ represent a measure of the similitude between the dilated parent wavelet and the signal $x(t)$ at scale a and time b. The mapping between scale factor a and frequency ω facilitates displaying wavelet coefficients in time-frequency plane.

The selection of an appropriate type of parent wavelet function is crucial for the effectiveness of CWT. Though there are many parent wavelets used in practice, of both discrete and continuous form, this paper shall focus on the complex Morlet wavelet transform. In mathematics, complex Morlet wavelet is a wavelet composed of a complex exponential carrier multiplied by a Gaussian window(Bernardino and Santos-Victor 2007), and the mathematical expression of this wavelet is

$$\psi_{\sigma}(t) = c_{\sigma}\pi^{-\frac{1}{4}}e^{-\frac{t^2}{2}}\left(e^{-i\sigma t} - \kappa_{\sigma}\right) \tag{3}$$

where $\kappa_{\sigma} = e^{-\frac{\sigma^2}{2}}$ is defined by the admissibility criterion and the normalisation constant c_{σ} is

$$c_{\sigma} = (1 + e^{-\sigma^2} - 2e^{-\frac{3\sigma^2}{4}})^{-\frac{1}{2}} \tag{4}$$

The Fourier transform of the complex Morlet wavelet is

$$\hat{\psi}_{\sigma}(\omega) = c_{\sigma}\pi^{-\frac{1}{4}}\left(e^{-\frac{(\sigma-\omega)^2}{2}} - \kappa_{\sigma}e^{-\frac{\omega^2}{2}}\right) \tag{5}$$

The value of σ determines the value of the central frequency F_c and the frequency bandwidth F_b. F_c is the position of the global maximum of $\hat{\psi}_{\sigma}(\omega)$ which is given by the solution of Eq. (6)

$$(F_c - \sigma)^2 - 1 = \left({F_c}^2 - 1\right)e^{-\sigma F_c} \tag{6}$$

The parameter σ in the complex Morlet wavelet allows trade between time and frequency resolutions. As a result, one can obtain the optimum resolution by changing the value of σ continuously. Sparsity of wavelet coefficients is usually used as the rule for evaluating the wavelet base, and it can be measured with wavelet entropy (Lin and Qu 2000). Therefore, in this study, the optimal value of parameter σ is obtained by finding the minimal value of wavelet entropy.

2.2 Synchrosqueezing wavelet transform

A practical time-varying response signal usually includes several components, and each component has its own local features, such as instantaneous frequency. The definition of instantaneous frequency is the derivative of the phase of the analytical signal, whose real part and imaginary part are real signal itself and its Hilbert transform, respectively. The objective of the synchrosqueezing wavelet transform is to extract instantaneous frequency by characterizing time frequency plane. Set a typical time varying signal as the sum of *n* IMFs and a residual (Huang *et al*. 1998, 1999).

$$x(t) = \sum_{i=1}^{n} x_i(t) + r(t) \tag{7}$$

in which, each IMF $x_i(t) = A_i(t)\cos\left(\phi_i(t)\right)$ is an oscillating function. $A_i(t)$ and $\phi_i(t)$ represent time-varying amplitude and phase angle respectively. The change in time of $A_i(t)$ and ${\phi'}_i(t)$ is much slower than the change of $x(t)$ itself, and $r(t)$ represents noise or observation error. What we need to do is extracting the amplitude factor $A_i(t)$ and instantaneous frequency ${\phi'}_i(t)$ for each *i* by refining time frequency curves.

Signals of Eq. (7) arise naturally in the area of civil engineering. After performing CWT of a vibration signal, several different algorithms (Kijewski and Kareem 2003, Hou *et al*. 2006) can be employed to support wavelet ridge extraction. Nevertheless, a meaningful research (Daubechies and Maes 1996) indicates that wavelet coefficients itself is an oscillating function of time even for the simplest harmonic wave function. If the parent wave function ψ has fast decay, its Fourier transform $\hat{\psi}(\xi)$ is approximately equal to zero in the negative frequencies: $\hat{\psi}(\xi) = 0$, for $\xi < 0$, and is concentrated around $a = \omega_0/\omega$. Take $x(t) = A\cos(\omega t)$ for example, and we can rewrite wavelet coefficients $W_x(a, b)$ by Plancherel's theorem, as

$$W_x(a,b)=\frac{1}{2\pi}\int \hat{x}\,(\xi)\sqrt{a}\overline{\hat{\psi}(a\xi)}e^{ib\xi}\mathrm{d}\xi\ =\frac{A}{4\pi}\int[\delta(\xi-\omega)+\delta(\xi+\omega)]\sqrt{a}\overline{\hat{\psi}(a\xi)}e^{ib\xi}\mathrm{d}\xi$$
$$=\frac{A}{4\pi}\sqrt{a}\overline{\hat{\psi}(a\omega)}e^{ib\omega} \tag{8}$$

in which, $\hat{x}(\xi)$ is the Fourier transform of signal $x(t)$, $\hat{\psi}(\xi)=\frac{1}{\sqrt{2\pi}}\int_{-\infty}^{\infty}\psi(t)\,e^{-i\xi t}\mathrm{d}t$ represents ψ in frequency domain. Debechies and Maes (1996) indicates that although $W_x(a,b)$ is spread out in scale a, its oscillatory behavior in time b points to the original frequency ω, no matter what the value of a would be. Consequently, the instantaneous frequency is preliminarily estimated by taking derivatives of wavelet coefficients. The formula of the computation is shown as

$$\omega_x(a,b)=\begin{cases}\frac{-i\partial_b W_x(a,b)}{W_x(a,b)} & |W_x(a,b)|>0\\ \infty & |W_x(a,b)|=0\end{cases} \tag{9}$$

In the synchrosqueezing step, the energy from time-scale plane is transferred to the time-frequency plane according to a map between (a,b) and $(\omega_x(a,b),b)$. The frequency variable ω and scale factor a were "binned", namely discretized, i.e., $W_x(a,b)$ was computed only at discrete points a_i, with $a_i-a_{i-1}=(\Delta a)_i$, and its synchrosqueezing value was likewise determined merely at the centers ω_l of successive bins $[\omega_l-\frac{1}{2}\Delta\omega,\omega_l+\frac{1}{2}\Delta\omega]$, with $\omega_l-\omega_{l-1}=\Delta\omega$. Therefore, the synchrosqueezing wavelet transform of $x(t)$ is expressed as

$$T_x(\omega_l,b)=\sum_{a_i:|\omega_x(a_i,b)-\omega_l|\le\Delta\omega/2}W_x(a_i,b)a_i^{-3/2}\,(\Delta a)_i \tag{10}$$

If frequency ω and scale a are treated as continuous variables, the analog of the Eq. (10) is

$$T_x(\omega,b)=\int_{a:|\omega_x(a,b)-\omega_l|\le\Delta\omega/2}W_x(a,b)a^{-3/2}\,\mathrm{d}a \tag{11}$$

In practice, Thakur *et al*. (2013) noted that the discrete wavelet transform samples the CWT coefficient $W_x(a,b)$ at the locations (a_i,b), where $a_i=2^{i/n_v}, i=1,\ldots,Ln_v$, L is a nonnegative integer and controls the interest largest scale value, the number of voices n_v is a user-defined parameter that controls the number of scales and its value was recommended as 32. Then, the discrete wavelet transform coefficient is given with respect to $n_a=Ln_v$ log-scale samples of the scale a, and this leads to some considerations on estimating T_x. First, due to the lower resolutions in the lower frequencies (larger scales), the frequency domain is divided into n_a components on a log scale. Second, the transform $a(i)=2^{i/n_v}$, $da(i)=a\frac{\log(2)}{n_v}\mathrm{d}i$, leads to the modification integrand $W_x(a,b)a^{-1/2}\frac{\log(2)}{n_v}\mathrm{d}i$ in Eq. (11). Since $\Delta i=1$, the discrete synchrosqueezing wavelet transform $T_x(\omega_l,b)$ of Eq. (10) can be further calculated as

$$T_x(\omega_l,b)=\sum_{a_i:\omega_x(a_i,b)\in[\omega_l-\frac{1}{2}\Delta\omega,\ \omega_l+\frac{1}{2}\Delta\omega]}W_x(a_i,b)a_i^{-1/2}\frac{\log(2)}{n_v} \tag{12}$$

in which, $\omega_l=2^{l\Delta\omega}\frac{1}{m\Delta t}$ $(l=0,1,2,\ldots,n_a-1)$ for a signal $x(t)$ is discretized over an interval of length $m\Delta t$. Δt is the discretization period, m is total number of discretization points and its log2 value should be a nonnegative integer, and $\Delta\omega=\frac{1}{n_a-1}\log_2\left(\frac{m}{2}\right)$.

As a result, signals with the expression of Eq. (7) will have a frequency image $|T_x(\omega_l,b)|$ composed of several curves in the time-frequency plane. The instantaneous frequency curves can be extracted by maximizing a functional of the energy of the curve.

Unlike most TFR methods, synchrosqueezing wavelet transform allows individual reconstruction of component signals. In other words, synchrosqueezing wavelet transform is invertible. It is expressed by Eqs. (13) and (14) that the original signal can be reconstructed after synchrosqueezing wavelet transform is performed.

$$\begin{aligned}\int_0^{\infty} W_x(a,b)a^{-3/2}\,\mathrm{d}a &= \frac{1}{2\pi}\int_{-\infty}^{\infty}\int_0^{\infty}\hat{x}(\xi)\overline{\hat{\psi}(a\xi)}e^{ib\xi}a^{-1}\mathrm{d}a\mathrm{d}\xi \\ &= \frac{1}{2\pi}\int_0^{\infty}\int_0^{\infty}\hat{x}(\xi)\overline{\hat{\psi}(a\xi)}e^{ib\xi}a^{-1}\mathrm{d}a\mathrm{d}\xi \\ &= \int_0^{\infty}\overline{\hat{\psi}(\zeta)}\frac{\mathrm{d}\zeta}{\zeta}\cdot\frac{1}{2\pi}\int_0^{\infty}\hat{x}(\xi)e^{ib\xi}\mathrm{d}\xi\end{aligned} \tag{13}$$

where $\hat{\psi}(\zeta)$ represents the Fourier transform of parent wavelet function $\psi(t)$, $\hat{\psi}(a\xi)$ is the complex conjugate of $\psi(a\xi)$. By defining a normalizing constant $C_\psi = \frac{1}{2}\int_0^{\infty}\overline{\hat{\psi}(\zeta)}\frac{\mathrm{d}\zeta}{\zeta}$, the original signal can be estimated as

$$x(b) = \Re\mathrm{e}\left[C_\psi{}^{-1}\left(\int_0^{\infty} W_x(a,b)a^{-3/2}\mathrm{d}a\right)\right] \tag{14}$$

where $\Re\mathrm{e}[\cdot]$ returns the real part of the objective function. In the piecewise constant approximation corresponding to the binning in a, Eq. (14) becomes

$$x(b) \approx \Re\mathrm{e}\left[C_\psi{}^{-1}\sum_i W_x(a,b)\,a_i{}^{-3/2}(\Delta a)_i\right] = \Re\mathrm{e}\left[C_\psi{}^{-1}\sum_l T_x(\omega_l,b)(\Delta\omega)\right] \tag{15}$$

Since a wide range of practical response signals accord with the assumptions given by synchrosqueezing algorithm, each component of analyzed signal can be estimated successfully, provided a sufficiently fine division of frequency bins $\{\omega_l\}$.

2.3 Time-varying damage index

Since structural damage often causes the changes of modal parameters, therefore, structural modal parameters such as frequency and mode shape or their combinations can be used for structural damage detection. As one of the candidate damage indices, structural modal flexibility is commonly used for structural damage detection (Pandey and Biswas 1994). With mode shapes normalized to unit mass, as $\boldsymbol{\Phi M \Phi^T} = \boldsymbol{I}$, The modal flexibility and its increment can be obtained from the modal data as

$$\boldsymbol{F} = \boldsymbol{\Phi\Omega^{-1}\Phi^T} = \sum_{i=1}^{N}\frac{\phi_i\,\phi_i{}^T}{\omega_i{}^2} \tag{16a}$$

$$\boldsymbol{\Delta} = \boldsymbol{F} - \boldsymbol{F}_d \tag{16b}$$

in which, $\boldsymbol{\Phi} = [\boldsymbol{\phi_1}\ \boldsymbol{\phi_2}\ \ldots\ \boldsymbol{\phi_N}]$ is the mass normalized mode shape matrix, the subscript i represents the i^{th} order mode. $\boldsymbol{M}$ and $\boldsymbol{I}$ are mass matrix and identity matrix, respectively. ω_i is the i^{th} order modal frequency and $\boldsymbol{\Omega} = \mathrm{diag}(\omega_i{}^2)$. N is the number of degree of freedom (DOF). $\boldsymbol{F}$ and $\boldsymbol{F_d}$ are modal flexibility matrices for the intact and the damaged cases, respectively. $\boldsymbol{\Delta}$ reflects the change of flexibility matrix, which can be used to detect structural damage. The modal flexibility matrix converges rapidly with the increase of modal frequency, and thus only a few low order modes suffice to make a good estimation of the flexibility matrix.

Recently, the modal flexibility index has been widely applied in the field of structural damage detection. However, it is difficult to obtain complete information about modal flexibility in practice, especially for structures suffering time-varying damage. Furthermore, it is hard to obtain the mass normalized mode shape. Inspired by the equations of modal flexibility damage index, we present a new time-varying damage index which just needs to know the instantaneous frequency and the modal participation factor ratio and does not require mass normalized mode shape.

Set displacement responses (similarly, other measured responses such as acceleration and velocity also can be used) of two nodes (s and l) are known, termed as $x_s(t)$ and $x_l(t)$. They can be simply expressed in the modal coordinates:

$$\begin{cases} x_s(t) = \phi_{s1}q_1 + \phi_{s2}q_2 + \phi_{s3}q_3 + \cdots + \phi_{sN}q_N \\ x_l(t) = \phi_{l1}q_1 + \phi_{l2}q_2 + \phi_{l3}q_3 + \cdots + \phi_{lN}q_N \end{cases} \tag{17}$$

in which, $[\phi_{s1}\ \phi_{s2}\ \phi_{s3}\ \ldots\ \phi_{sN}]$ and $[\phi_{l1}\ \phi_{l2}\ \phi_{l3}\ \ldots\ \phi_{lN}]$ represent the s^{th} and l^{th} row vectors of mode shape matrix, respectively. $[q_1\ q_2\ \ldots\ q_N]$ is the modal coordinate vector, and N denotes the number of DOF of the structure. Each IMF $\phi_{si}q_i$ or $\phi_{li}q_i$ from the measured responses can be reconstructed by the proposed syncrhrosqueezing wavelet transform, thus the analytic signal of each IMF can be defined as a complex function which has itself as real part and its Hilbert transform as imaginary part

$$\begin{cases} Z_{s1}(t) = \phi_{s1}q_1 + \mathrm{H}[\phi_{s1}q_1] = \phi_{s1}(t)A_{q_1}(t)e^{-j\theta_{q_1}(t)} \\ Z_{s2}(t) = \phi_{s2}q_2 + \mathrm{H}[\phi_{s2}q_2] = \phi_{s2}(t)A_{q_2}(t)e^{-j\theta_{q2}(t)} \\ Z_{l1}(t) = \phi_{l1}q_1 + \mathrm{H}[\phi_{l1}q_1] = \phi_{l1}(t)A_{q_1}(t)e^{-j\theta_{q_1}(t)} \\ Z_{l2}(t) = \phi_{l2}q_2 + \mathrm{H}[\phi_{l2}q_2] = \phi_{l2}(t)A_{q_2}(t)e^{-j\theta_{q2}(t)} \\ \quad\vdots \end{cases} \tag{18}$$

where H[•] denotes the Hilbert transform. With the node s as reference point (usually the position where the maximum response happens), the modal participation factor ratio of the first order mode between node l and node s, $\varphi_{l1,s1}$ can be defined as

$$\varphi_{l1,s1}(t) = \frac{\phi_{l1}(t)}{\phi_{s1}(t)} = \frac{\phi_{l1}(t)A_{q_1}(t)e^{-j\theta_{q_1}(t)}}{\phi_{s1}(t)A_{q_1}(t)e^{-j\theta_{q_1}(t)}} = \frac{|Z_{l1}(t)|}{|Z_{s1}(t)|} \tag{19}$$

Other modal participation factor ratio of higher order mode between node l and node s can be expressed in a similar way.

Once the instantaneous frequencies and modal participation factor ratios are obtained, a new time-varying damage index (TVDI) is defined as

$$\mathrm{TVDI}_l(t) = 1 - \frac{\sum_{i=1}^{N}\left[\frac{\varphi_{li,si}(t)}{\omega_i(t)}\right]^2}{\sum_{i=1}^{N}\left[\frac{\varphi_{li,si}^{d}(t)}{\omega_i^{d}(t)}\right]^2} \tag{20}$$

where $\omega_i(t)$ is the instantaneous frequency of the i^{th} order mode, $\varphi_{li,si}(t)$ is the modal participation factor ratio of the i^{th} order mode between node l and node s, N represents the number of DOF. The superscript d denotes the damage state. The new damage index TVDI indicates the degree of damage ranging from 0 (intact) to 1 (collapse). It should be noted that the modal participation factor ratio $\varphi_{li,si}(t)$ is not normalized to mass. Since the new damage index TVDI is a function of the ratio of $\varphi_{li,si}(t)$ to $\varphi^{d}_{li,si}(t)$, the scale caused by no mass-normalization will be removed in Eq. (20) on condition that the mass keep invariant during damage process.

3. Instantaneous frequency extraction

Classical Duffing equation is usually employed to simulate nonlinear motion of mass-spring-damper systems. A Duffing equation in this example is given as (Feldman 2011)

$$\ddot{x} + 0.05\dot{x} + k_1 x + k_2 x^3 = 0 \tag{21}$$

where linear stiffness k_1 and cubic stiffness k_2 are 1 and 0.01 respectively. The motion begins with $x_0 = 10$, $\dot{x} = 0$, and its response is simulated using 4th Runge-Kutta method with time interval of 0.1 seconds. Correspondingly, the Duffing system with forced vibration is adopted to establish the viability and effectiveness of synchrosqueezing wavelet transform. The excitation is set as Gaussian white noise with zero mean and 0.1g (gravitational acceleration) standard deviation. To study the effect of noise on instantaneous frequency extraction, 5% simulated Gaussian white noise is added to the displacement responses. The noise intensity is defined by the following signal-to-noise ratio (SNR)

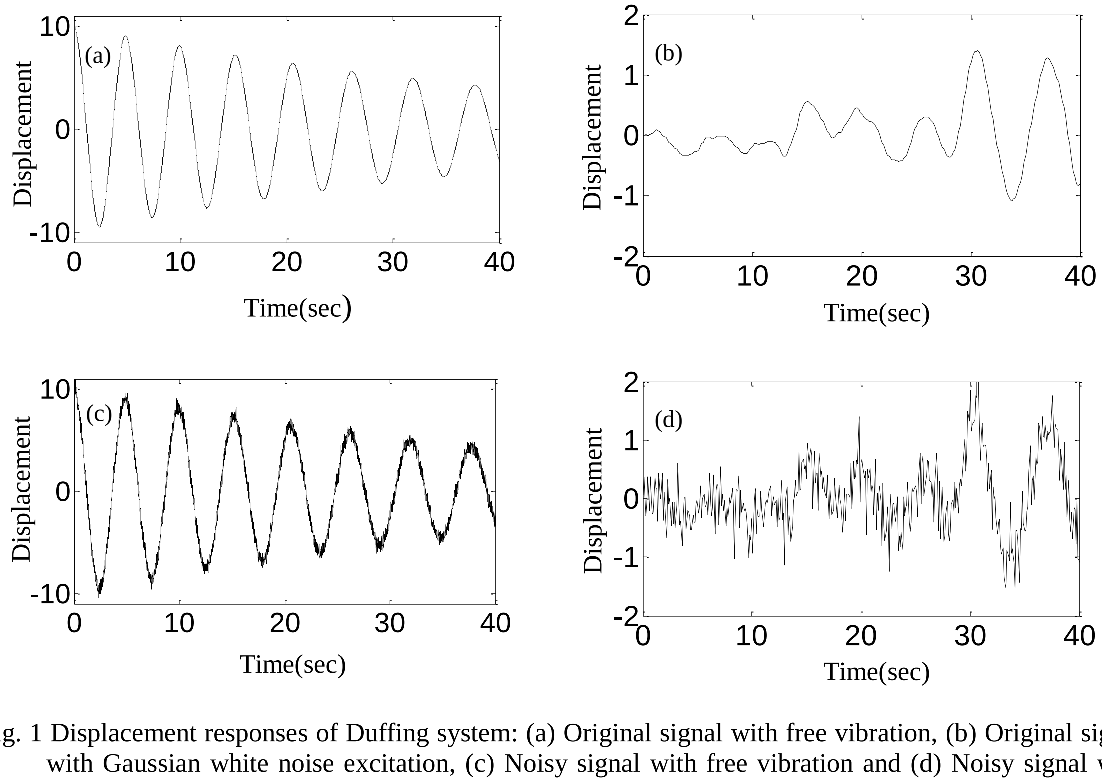

Fig. 1 Displacement responses of Duffing system: (a) Original signal with free vibration, (b) Original signal with Gaussian white noise excitation, (c) Noisy signal with free vibration and (d) Noisy signal with Gaussian white noise excitation

$$\mathrm{SNR} = 20\log_{10}\frac{A_{\mathrm{signal}}}{A_{\mathrm{noise}}} = 10\log_{10}\frac{A_{\mathrm{signal}}^2}{A_{\mathrm{noise}}^2} \quad \text{(in dB)} \tag{22}$$

where A_{signal} and A_{noise} refer to the root mean square value of the signal and the noise, respectively. Noise level means the ratio of A_{noise}^2 to A_{signal}^2. For example, SNR equals 13 dB according to Eq. (22) when 5% Gaussian white noise is simulated. Fig. 1 shows the displacement responses of the Duffing nonlinear system.

Synchrosqueezing wavelet transform is then performed to extract instantaneous frequency curves according to CWT of response signals. The extracted instantaneous frequency is plotted using a solid line, while the identified instantaneous frequency by extracting wavelet ridges is plotted using a dashed line in Fig. 2.

It can be clearly seen from Fig. 2 that the identified instantaneous frequency by synchrosqueezing wavelet transform decreases rapidly at the beginning and gradually approaches an asymptotic value (0.16 Hz) of the corresponding linear system. This phenomenon also means that cubic stiffness is dominant in large amplitude and then linear behavior stand out, with nonlinear effect gradually becoming unimportant. Compared with the results by wavelet transform method, synchrosqueezing wavelet transform improves the quality of time-frequency curves and avoid sawtooth phenomenon in wavelet transform, especially for signals contaminated by Gaussian white noise. In addition, the end effects of wavelet transform also has great impact on the identified instantaneous frequency at the beginning time. However, synchrosqueezing wavelet transform reduces the end effects to an extent owing to its stability.

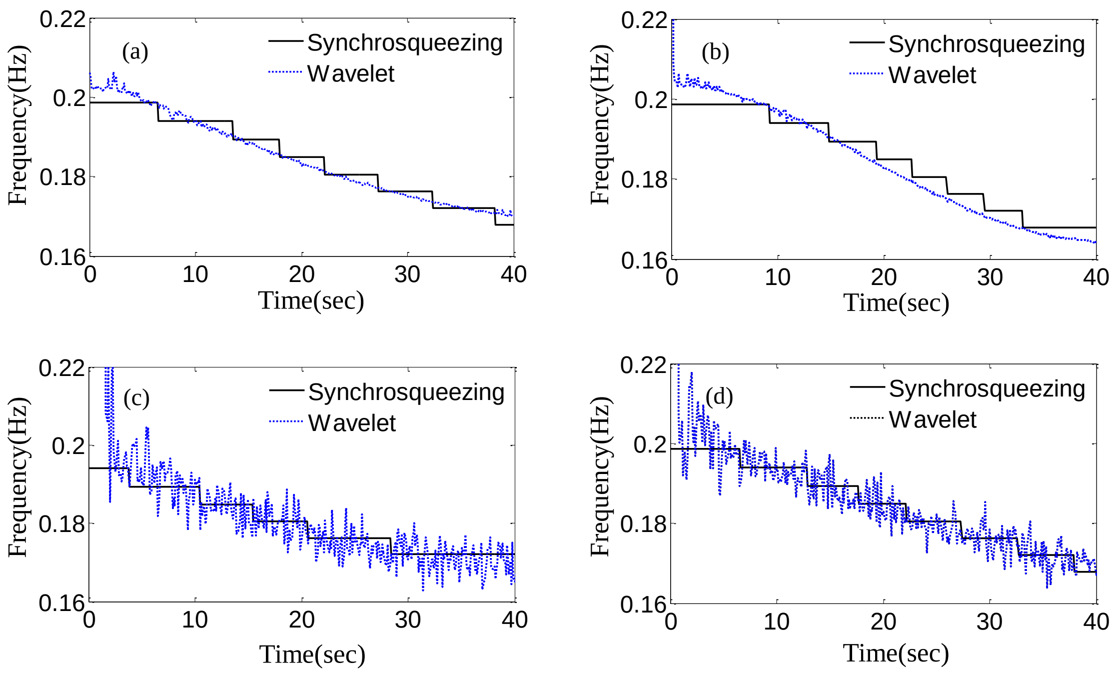

Fig. 2 Time-frequency spectrum of Duffing system: (a) Original signal under free vibration, (b) Original signal under Gaussian white noise excitation, (c) Noisy signal under free vibration and (d) Noisy signal under Gaussian white noise excitation

Therefore it is concluded that the new introduced synchrosqueezing wavelet transform method can extract instantaneous frequency more effectively and accurately than wavelet transform when Gaussian white noise is injected to the simulated displacement responses. The improvement for the accuracy of frequency extraction plays an important role on damage detection in the next section because the proposed time-varying damage index TVDI in Eq. (20) is mainly consist of instantaneous frequencies and modal participation factor ratio.

4. Damage detection

To verify the effectiveness of the proposed method, a simply supported beam with dimensions: width of cross section b=0.2 m, height of cross section h=0.2 m and length of the beam L=5 m is simulated. The material parameters are: the modulus of elasticity E=210Gpa and the mass density ρ=7800 kg/m^3. The finite element model of the beam is discretized to 20 equal length elements. The number of nodes and elements of the finite element model are marked in Fig. 3.

For single damage detection, four damage scenarios (DS1-DS4) are considered, which are described in Table 1. The structural damage is simulated by reducing Young's modulus at a particular element location. For DS1 and DS3, the free vibration of the simply supported beam is simulated, while the simply supported beam is subjected to 1940 El Centro earthquake excitation for DS2 and DS4. The direct integral calculus method of Newmark is used to simulate the displacement, velocity and acceleration responses of each node, with time interval of 0.02s. To consider the influence of noise, 5% simulated Gaussian white noise is added to the response signals. For simplicity, the responses of free vibration for DS3 and the responses to earthquake for DS4 are plotted in Fig. 4.

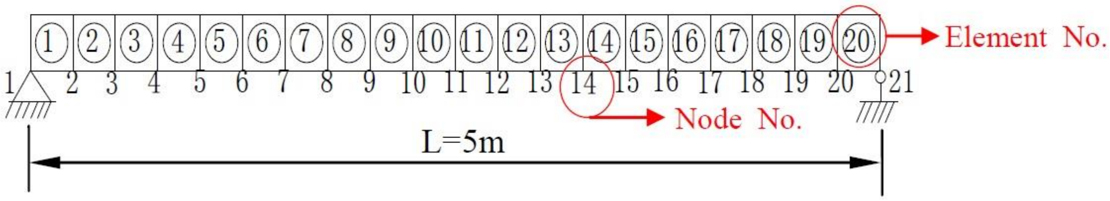

Fig. 3 A finite element model of the simply supported beam

Table 1 Four damage scenarios with single damage location

Damage scenario	Damage location	Stiffness reduction	Excitation
DS1	Element 5 and 6	reduce suddenly 40% at time t=2s	Free vibration
DS2	Element 5 and 6	reduce suddenly 40% at time t=2s	Earthquake ground motion
DS3	Element 5 and 6	reduce linearly 40% over period of t=2s and t=6s	Free vibration
DS4	Element 5 and 6	reduce linearly 40% over period of t=2s and t=6s	Earthquake ground motion

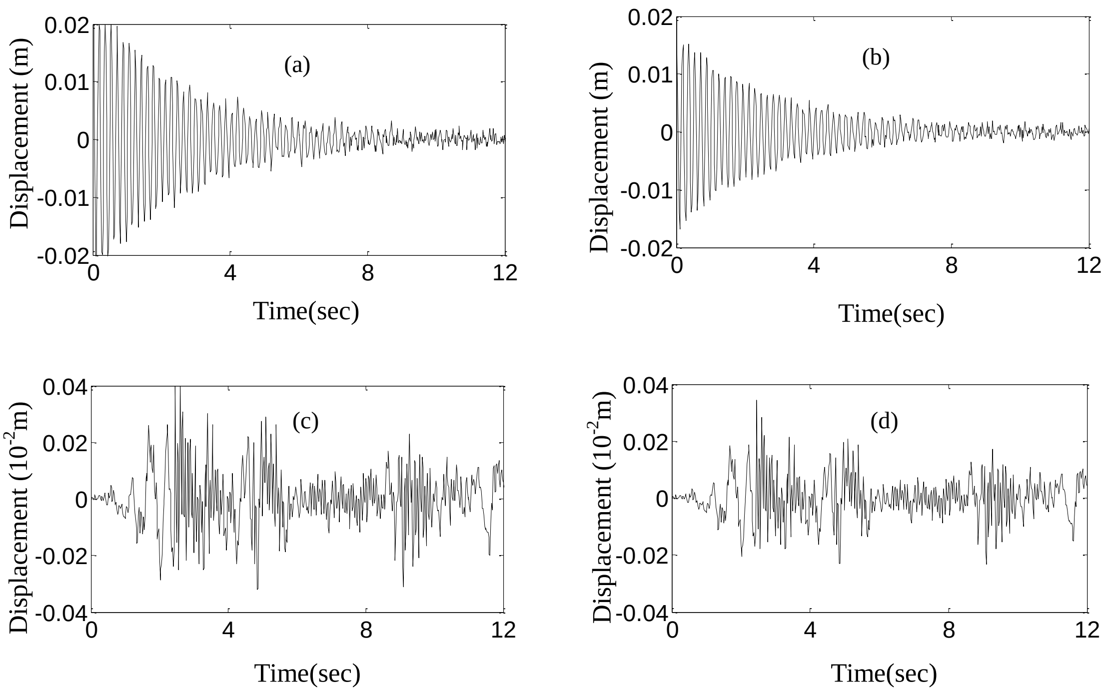

Fig. 4 Displacement response of simply supported beam without Gaussian white noise: (a) Node 11 in DS3, (b) Node 6 in DS3, (c) Node 11 in DS4 and (d) Node 6 in DS4

Synchrosqueezing wavelet transform is performed on displacement response of node 6 to extract the instantaneous frequency. Then set node 11 as reference point, and use IMFs reconstructed from displacement responses of nodes 6 and 11 to calculate the modal participation factor ratio of the first order mode according to Eq. (17) to (19). The same method is employed to extract the instantaneous frequency and modal participation factor ratio for intact scenario. Then the values of TVDI can be calculated using Eq. (20). Fig. 5 shows the values of TVDI for four damage scenarios. It can be clearly seen from Fig. 5, the proposed damage index effectively detect the occurrence of damages, whether the stiffness reduces suddenly or linearly. The sudden increase of TVDI at time point t=2s in Figs. 5(a) and 5(b) is linked to the sudden 40% stiffness reduction at the same time point. Accordingly, as presented in Figs. 5(c) and 5(d), the linear reduction of stiffness over a period between t=2s and t=6s results in that the value of TVDI increases linearly during the same time period. It can also be found that the added Gaussian white noise has some impact on damage detection results. However, the occurrence of damage can still be accurately detected. As shown in Fig. 5, the values of TVDI do not always equal to zero before the abrupt or linear damage is inflicted. The main reason for this phenomenon is the end effects of wavelet transform. End effects can also be found in the final seconds of response signals. For example, there are some increasing and decreasing of values of TVDI in Figs. 5(a) and 5(c) during t=10s to t=12s. For free vibration, there is another reason accounting for the change of TVDI between t=10s and t=12s. The amplitude of displacement response under free vibration gradually decreases to noise level even approximates to zero, which leads to low signal to noise ratio. As a consequence, the effectiveness and accuracy of the instantaneous frequency identification and the modal participation factor ratio extraction will be influenced to an extent, and thus the calculated TVDI exhibits oscillatory behavior. However, the proposed method can still effectively track the time-varying damage except at the beginning and end of vibration.

To further verify the effective of the proposed method for multiple damage evolution detection, the above mentioned simply supported beam with two damage locations is considered. Stiffness of elements 5 and 6 reduces linearly 40% over the period of t=2s and t=6s, while 40% stiffness reduction is imposed on elements 15 and 16 at time point t=9s. The 1940 El Centro earthquake is used as external excitation and Newmark integration method is employed to simulate the displacement responses of all 21 nodes with time interval of 0.02s. Displacement responses of nodes 6 and 16 are selected to extract instantaneous frequencies by using synchrosqueezing wavelet transform. Just like scenarios with single damage location, node 11 is set as reference point, and IMFs reconstructed from displacement responses of nodes 6 and 11 are used to calculate the modal participation factor ratio of the first mode between node 6 and node 11 according to Eq. (19). Similarly, IMFs reconstructed from displacement responses of node 16 and node 11 are used to calculate the modal participation factor ratio of the first mode between node 16 and node 11.

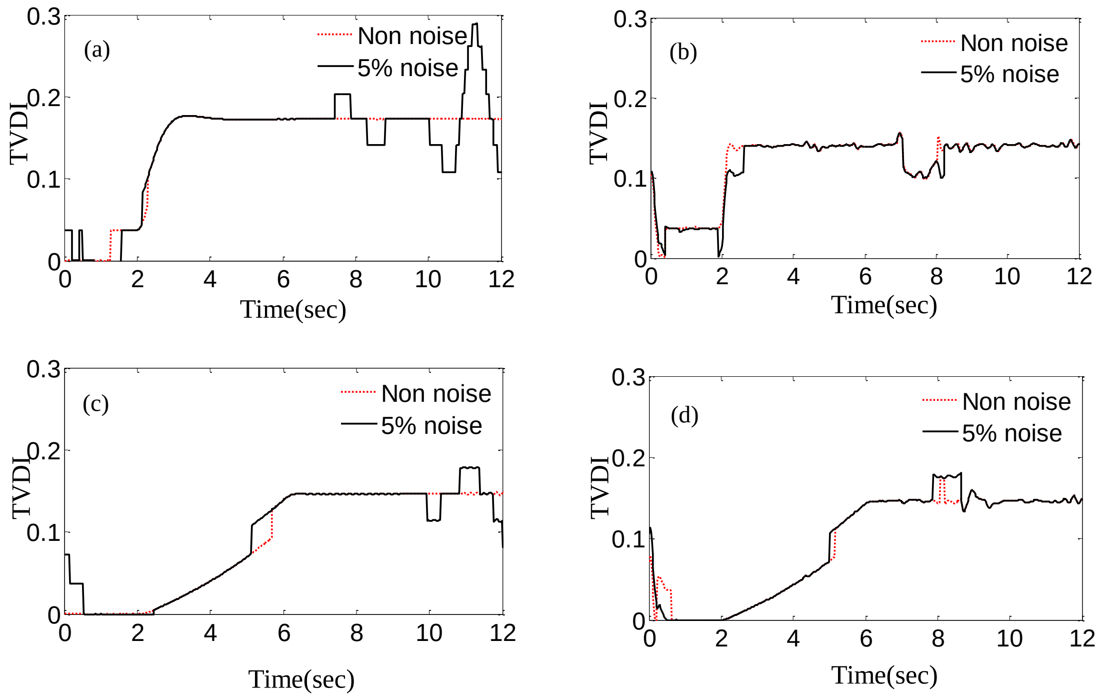

Fig. 5 Damage identification results for different damage scenarios: (a) DS1, (b) DS2, (c) DS3 and (d) DS4

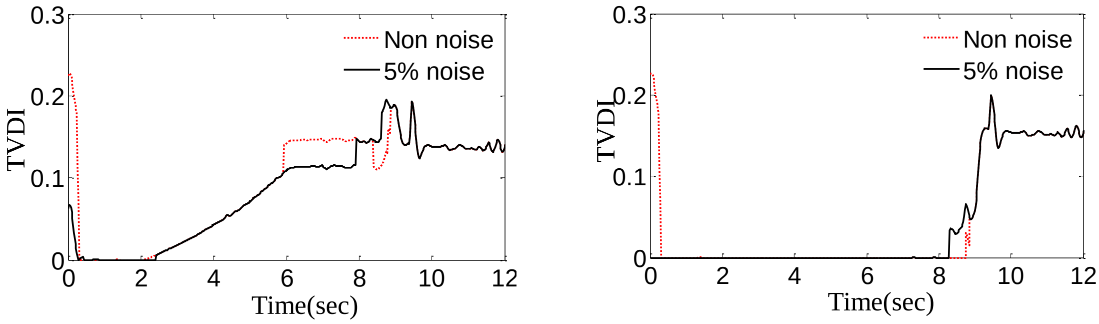

(a) TVDI at Node 6 (b) TVDI at Node 16

Fig. 6 Damage identification results of the simply supported beam with two damage locations

The extraction of instantaneous frequencies and modal participation factor ratio for intact scenario follows a similar process. Then the values of TVDI at nodes 6 and 16 can be solved by Eq. (20), respectively. The variations of TVDI over time are presented in Fig. 6. As one can see from Fig. 6, Linear stiffness reduction of Element 5 and 6 between t=2s and t=6s and sudden stiffness reduction of element 15 and 16 at t=9s are basically reflected by the variation of TVDI in Fig. 6(a) and 6(b), respectively. The phenomenon that the values of TVDI do not always equal to zero before damage is inflicted also exists in Fig. 6(a) and 6(b). End effects of synchrosqueezing wavelet transform account for this phenomenon. The presence of the Gaussian white noise decreases the accuracy of damage detection, nevertheless, the trend of stiffness reduction at node 6 and node 16 seems not affected. Therefore, it is feasible to use TVDI for tracking the damage evolution of simply supported beam with two or multiple damage locations.

5. Conclusions

In this paper, synchrosqueezing wavelet transform is introduced to extract instantaneous frequency and reconstruct IMFs from the measured responses of structures with time-varying damage. Then the instantaneous modal participation factor ratio is further identified from the reconstructed IMFs. Based on the instantaneous frequency and modal participation factor ratio, the TVDI is defined as a new damage index for the time varying damage detection. A Duffing nonlinear system and a simply supported beam with free and forced vibrations are simulated as numerical examples. Based on the numerical results, the following conclusions can be drawn:

(1) The instantaneous frequency can be directly extracted for Duffing nonlinear systems subjected impulsive loads or Gaussian white noise excitations by using the proposed synchrosqueezing wavelet transform.
(2) The defined TVDI can effectively detect abrupt or linear time-varying single damage for beam structures, even when response signals are contaminated by Gaussian white noise.
(3) From the simulation of the simply support beam, the defined TVDI can also effectively detect multiple damages in beams subjected to earthquake excitations.

Acknowledgments

This study is sponsored by the National Natural Science Foundation of China (NSFC) under Grants No.51078357 and No.51208165. The results and opinions expressed in this paper are those of the authors only.

References

Bernardino, A. and Santos-Victor, J. (2005), "A real-time Gabor primal Sketch for visual attention", *IBPRIA-2nd Iberian Conference on Pattern Recognition and Image Analysis*, Estoril, Portugal.

Chen, G.D. and Wang, Z.C. (2012), "A signal decomposition theorem with Hilbert transform and its application to narrowband time series with closely spaced frequency components", *Mech. Syst. Signal Pr.*, **28**, 258-279.

Daubechies, I. and Maes, S. (1996), *A nonlinear squeezing of the continuous wavelet transform based on nerve models*, (Eds., A. Aldroubi and M. Unser),Wavelets in Medicine and Biology, CRC Press.

Daubechies, I., Lu, J.F. and Wu, H.T. (2011), "Synchrosqueezed wavelet transforms: An empirical mode decomposition-like tool", *Appl. Comput. Harmon. A.*, **2**(30), 243-261.

Doebling, S.W., Farrar, C.R. and Prime M.B. (1998). "A summary review of vibration-based damage identification methods", *Shock Vib. Dig.*, **30** (2), 91-105.

Fayyadh, M.M., Razak, H.A. and Ismail, Z. (2011), "Combined modal parameters-based index for damage identification in beamlike structures: theoretical development and verification", *Arch. Civil Mech. Eng.*, **11**(3), 587-609.

Feldman M. (2011), "Hilbert transform applications in mechanical vibration", *Mech. Syst. Signal Pr.*, **25**(3), 735-802.

Golmohamadi, M., Badri, H. and Ebrahimi, A. (2012), "Damage diagnosis in bridges using wavelet", Proceedings of the *IACSIT Coimbatore Conferences*, Singapore.

Hou, Z.K., Hera, A, and Shinde, A. (2006), "Wavelet-based structural health monitoring of earthquake excited structures", *Comput. -Aided Civil Infrastruct. Eng.*, **21**,268-279.

Huang, N.E. and Shen, S.S.P. (2005), *Hilbert-Huang transform and its application*, *World Scientific Publishing Company*, London.

Huang, N.E., Shen, Z. and Long, S.R. (1999), "A new view of nonlinear water waves: the Hilbert spectrum", *Annual Rev. Fluid Mech.*, **31**,417-457.

Huang, N.E., Shen, Z., Long, S.R., Wu, M.C., Shih, H.H., Zheng, Q., Yen, N.C., Tung, C.C. and Liu, H.H. (1998), "The empirical mode decomposition and the Hilbert spectrum for nonlinear and non-stationary time series analysis", *P. R. Soc. Lond. A*, **454**(1971), 903-995.

Jaishi, B. and Ren, W.X. (2006), "Damage detection by finite element model updating using modal flexibility residual", *J. Sound Vib.*, **290**(1-2), 369-387.

Kijewski, T. and Kareem, A. (1999), "Applications of wavelet transform in earthquake, wind and ocean engineering ", *Eng. Struct.*, **21**(2),149-167.

Kijewski, T. and Kareem, A. (2003). "Wavelet transforms for system identification in civil engineering", *Comput.-Aided Civil Infrastruct. Eng.*, **18**(5), 339-355.

Kijewski, T. and Kareem, A. (2007), "Nonlinear signal analysis: time-frequency perspectives", *J. Eng. Mech.*, **133**(2), 238-245.

Kopsaftopoulos, F.P. and Fassois S.D. (2013), "A functional model based statistical time series method for vibration based damage detection, localization, and magnitude estimation", *Mech. Syst. Signal Pr.*, **39**(1-2), 143-161.

Li, C. and Liang, M. (2012a), "A generalized synchrosqueezing transform for enhancing signal time–frequency representation ", *Mech. Syst. Signal Pr.*, **9**(92), 2264-2274.

Li, C. and Liang, M. (2012b), "Time-frequency signal analysis for gearbox fault diagnosis using a generalized synchrosqueezing transform”, *Mech. Syst. Signal Pr*., **1**(26), 205-217.

Lin, J. and Qu, L. (2000), “Feature extraction based on morlet wavelet and its application for mechanical fault diagnosis”, *J. Sound Vib*., **234**(1), 135-148.

Mallat, S. (1999), *A wavelet tour of signal processing*, Academic Press, New York.

Pandey, A.K. and Biswas, M. (1994), “Damage detection in structures using changes in flexibility”, *J. Sound Vib.*, **169**(1), 3-17.

Rucka, M. (2011), “Damage detection in beams using wavelet transform on higher vibration modes”, *J. Theor. Appl. Mech*, **49**(2), 399-417.

Ruzzene, M., Fasana, A., Garibaldi, L. and Piombo, B. (1997), “Natural frequencies and dampings identification using wavelet transform: application to real data”, *Mech. Syst. Signal Pr.*, **11**(2), 207-218.

Thakur, G., Brevdo, E., Fučkar, N.S. and Wu, H.T. (2013), “The Synchrosqueezing algorithm for time-varying spectral analysis: Robustness properties and new paleoclimate applications”, *Signal Process*, **93**(5), 1079-1094.

Wang, J., Lin, C. and Yen, S. (2007), “A story damage index of seismically-excited buildings based on modal frequency and mode shape”, *Eng. Struct.*, **29**(9), 2143-2157.

Wu, H.T., Flandrin, P. and Daubechies, I. (2011), “One or two frequencies? The synchrosqueezing answers”, *Adv. Adap. Data Anal.*, **13**, 29-39.

Wu, Z.H. and Huang, N.E. (2009), “Ensemble empirical mode decomposition: a noise-assisted data analysis method”, *Adv. Adap. Data Anal.*, **1**(1), 11-41.

Xu, X., Shi, Z.Y. and You, Q. (2012), “Identification of linear time-varying systems using a wavelet-based state-space method”, *Mech. Syst. Signal Pr.*, **26**, 91-103.

Yan, W.J., Ren, W.X. and Huang, T.L. (2012), “Statistic structural damage detection based on the closed-form of element modal strain energy sensitivity”, *Mech. Syst. Signal Pr.*, **28**,183-194.

Yan, Y.J., Cheng L., Wu, Z.Y. and Yam, L.H. (2007), “Development in vibration-based structural damage detection technique”, *Mech. Syst. Signal Pr.*, **21**(5), 2198-2211.

Yang, Q.W. and Liu, J.K. (2006), “A coupled method for structural damage identification”, *J. Sound Vib.*, **296**(1-2),401-440.

Yang, Z. and Wang, L. (2010). “Structural damage detection by changes in natural frequencies”, *J. Intel. Mater. Syst. Str.*, **21**, 309-319.